Table II. Atomic Positions and B_{eq} for Compound Ib

atom	*x*	*y*	*z*	B_{eq}, Å^2
Au1	0.93096	0.21215	0.41116 (4)	3.65 (2)
I1	1.2111 (1)	-0.0105 (2)	0.45534 (8)	4.73 (5)
C1	1.051 (3)	0.362 (3)	0.308 (2)	5.4 (8)
C2	0.0705 (3)	0.389 (3)	0.382 (2)	7 (1)
F1	0.956 (2)	0.391 (3)	0.219 (1)	14 (1)
F2	1.116 (4)	0.502 (3)	0.341 (2)	17 (2)
F3	1.178 (3)	0.288 (3)	0.284 (2)	18 (2)
F4	0.752 (3)	0.557 (2)	0.405 (2)	13 (1)
F5	0.629 (2)	0.382 (2)	0.288 (1)	12 (1)
F6	0.594 (3)	0.389 (3)	0.382 (2)	7 (1)

Table III. Bond Distances (Å) and Angles (deg) for Compound Ib

	Distances		
Au1-C1	2.07 (2)	Au1-C2	2.12 (2)
Au1-I1	2.654 (1)	Au1-I1′	2.658 (1)
C1-F1	1.26 (2)	C1-F2	1.18 (2)
C1-F3	1.20 (3)	C2-F4	1.30 (2)
C2-F5	1.26 (2)	C2-F6	1.22 (3)
	Angles		
C1-Au1-C2	89.9 (9)	C1-Au1-I1	91.9 (6)
C1-Au1-I1′	177.7 (6)	C2-Au1-I1	177.8 (6)
C2-Au1-I1′	92.4 (6)	I1-Au1-I1′	85.74 (3)
F2-C1-F3	100 (2)	F2-C1-F1	108 (2)
F2-C1-Au1	116 (2)	F3-C1-F1	100 (2)
F3-C1-Au1	114 (1)	F1-C1-Au1	116 (1)
F6-C2-F5	107 (2)	F6-C2-F4	106 (2)
F6-C2-Au1	112 (1)	F5-C2-F4	109 (2)
F5-C2-Au1	111 (2)	F4-C2-Au1	111 (2)

Crystals of Ia were of poor quality with a low percentage of observed data, but unit cell constants (a = 7.444(8) Å, b = 7.20 (2) Å, c = 12.41 (4) Å, β = 99.0 (2)°) and preliminary structure solution showed Ia to be isomorphous to Ib. Because of the limited data quality, those results are not presented here. Data collection and refinement parameters for Ib are provided in Table I. The structure was solved by using the program MITHRIL[7] and refined to convergence by using TEXSAN (version 2.0).[8] The data were corrected for LP and polarization effects and absorption (empirical ψ scans).

Results and Discussion

The reaction of gold atoms with CF_3X, where X = Br or I, produces bis(trifluoromethyl)halogold complexes that exist as dimers in the solid state and in the gas phase. Ib (Figure 1) contains two gold atoms each of which is ligated by two trifluoromethyl groups and connected to each other via two bridging iodide ligands in a fashion similar to that of other known nonfluorinated alkylgold halides. The gold atoms have a square-planar geometry with the sum of the bond angles about the metal being 359.94°. The molecule is situated such that the center of the Au_2X_2 parallelogram is a crystallographic inversion center. There is no Au-Au bond. The fluorine atoms show some disorder about the 3-fold axis of the CF_3 moiety as is common for this group. Atomic positions and B_{eq} values are provided in Table II, while bond angles and distances are given in Table III. The Au-C distances are comparable to those found for other square-planar alkyl- and arylgold complexes such as $[Br_2Au(\mu\text{-}Br)_2AuMe_2]$ (2.12 (1) Å),[9] $[Au(CH_2)_2PPh_2]_2(CF_3)_2$ (2.140 (7) Å),[4] $[Me_2AuOH]_4$ (2.05 Å average),[10] $Au_2[(CH_2)_2PPh_2]_2(Me)Br$ (2.159 (2) Å),[11] $Au(C_6F_5)_2Cl(PPh_3)$ (2.12 (9), 2.18 (10) Å),[12] etc.[13]

This work represents the first structural characterization of stable unsubstituted (trifluoromethyl)gold halide compounds produced via metal atom reactions and indicates that such simple compounds are not inherently unstable. Previous work with (trifluoromethyl)gold complexes formed by atom vapor reactions employed PMe_3 to stabilize the product $Au(CF_3)_3$.[3] Bis(trifluoromethyl)gold halide dimers have recently been prepared[5], but the synthetic route was not straightforward, involving first synthesis of CF_3AuL followed by reaction with CF_3I, which was shown to follow a radical pathway. CF_3Br was unreactive under these conditions. Thus, the atom reactor synthesis represents at the moment the only known method to unsubstituted (trifluoromethyl)gold halide complexes, but the stability of these compounds suggests that other higher yield synthetic routes might be found.

Acknowledgment. We thank the Robert A. Welch Foundation and the U.S. Department of Energy for support of this research. The National Science Foundation is also acknowledged for financial assistance in the purchase of the single-crystal X-ray diffractometer.

Registry No. Ia, 123204-35-3; Ib, 123204-36-4; CBr_3I, 14349-80-5; CF_3I, 2314-97-8; Au, 7440-57-5.

Supplementary Material Available: Tables of crystallographic data collection and refinement parameters and anisotropic thermal parameters (2 pages); a listing of observed and calculated structure factors (9 pages). Ordering information is given on any current masthead page.

(7) Gilmore, G. *Mithril: A Computer Program for the Automatic Solution of Crystal Structures from X-ray Data*; University of Glasgow: Glasgow, Scotland, 1983.
(8) *TEXSAN (2.0) Program for Crystal Structure Determination and Refinement*; Molecular Structure Corp.: The Woodlands, TX. Scattering factors: Cromer, D. T.; Waber, J. T. *International Tables for X-ray Crystallography*; Kynoch Press: Birmingham, England, 1974; Vol. IV, pp 71 (scattering factors), 148 (anomalous dispersion) (current distributor Kluwer Academic Publishers, Dordrecht, The Netherlands).
(9) Komiya, S.; Huffman, J. C.; Kochi, J. *Inorg. Chem.* **1977**, *16*, 1253.
(10) Glass, G. E.; Konnert, J. H.; Miles, M. G.; Button, D.; Tobias, R. E. *J. Am. Chem. Soc.* **1968**, *90*, 1131.
(11) Basil, J D.; Murray, H. H.; Fackler, J. P., Jr.; Tocher, J.; Mazany, A. M.; Trzcinska-Bancroft, B.; Knachel, H.; Dudis, D.; Delord, T. J.; Marler, D. O. *J. Am. Chem. Soc.* **1985**, *107*, 6908.
(12) Baker, R. W.; Pauling, P. *Chem. Commun.* **1969**, 745.
(13) For a more extensive review of organogold compounds, see: (a) Schmidbaur, H. *Gmelin Handbuch für Anorganische Chemie. Organogold Compounds*; Springer Verlag: Berlin, 1980. (b) Puddephat, R. J. *The Chemistry of Gold*; Elsevier: New York, 1978.

Contribution from the Departments of Chemistry, University of California, Davis, California 95616, and University of Wrocław, Wrocław, Poland

Nuclear Magnetic Resonance Studies of Hydroquinone Dianion Bridged Iron(III) Porphyrin Dimers†

Alan L. Balch,*,‡ Rebecca L. Hart,‡ and Lechosław Latos-Grażyński§

Received November 27, 1989

The reaction of iron(III) arylporphyrin complexes, $(P)Fe^{III}Ar$, with dioxygen produces a variety of products, which depend on the reaction conditions.[1] One of these is the dimer $(P)Fe^{III}(1,4\text{-}OC_6H_4O)Fe^{III}(P)$, a species previously isolated and characterized in the solid state by Kessel and Hendrickson.[2,3] Such dimers are readily prepared by the reaction of an iron(II) complex with a *p*-benzoquinone (eq 1).[2-4] Mössbauer spectra indicate that

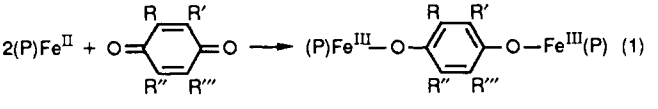

(1)

these are high-spin ($S = {}^5/_2$) iron(III) species.[2] Magnetic susceptibility studies show evidence of weak antiferromagnetic exchange with J values between -3.6 and -15.5 cm^{-1}.[2] Consequently, it may be anticipated that their ^{1}H NMR spectra will resemble those of high-spin iron(III) porphyrin complexes[5-7] rather than those of the much more strongly antiferromagnetically coupled μ-oxo compounds $(P)Fe^{III}OFe^{III}(P)$, where J is about -150 cm^{-1}.[8,9] In order to facilitate the detection of the diiron complexes and

† Abbreviations used: P, porphyrin dianion; TTP, tetra-*p*-tolylporphyrin dianion; OEP, octaethylporphyrin dianion; Ar, aryl group.
‡ University of California.
§ University of Wrocław.

0020-1669/90/1329-3253$02.50/0

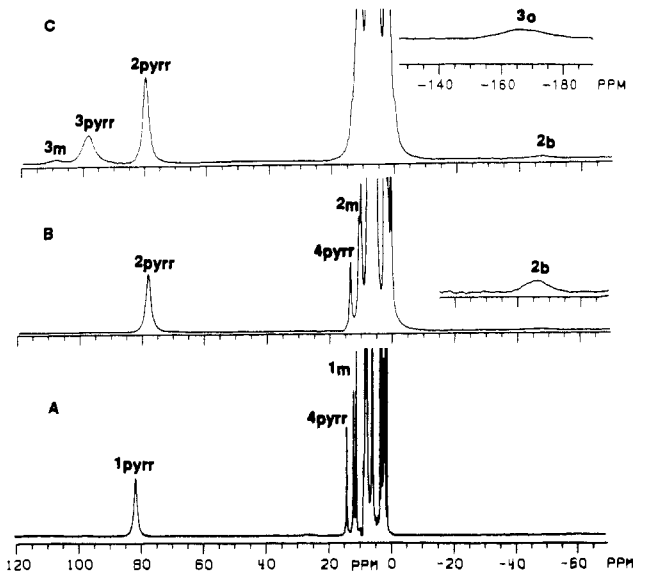

Figure 1. 360-MHz ^{1}H NMR spectra in toluene-d_8 at −30 °C of (A) (TTP)Fe^{III}(1,4-OC$_6$Cl$_4$O)Fe^{III}(TTP), 1, and (B) (TTP)Fe^{III}(1,4-OC$_6$H$_4$O)Fe^{III}(TTP), 2. (C) Reaction mixture obtained by treating (TTP)Fe^{III}OFe^{III}(TTP) with *p*-hydroquinone in toluene-d_8 at 30 °C. Resonances of (TTP)Fe^{III}(1,4-OC$_6$H$_4$OH) are labeled 3; those of (TTP)Fe^{III}OFe^{III}(TTP) are labeled 4. Subscripts indicate the proton location: pyrr, pyrrole; b, protons of the bridging ligand; m, meta (*p*-tolyl) protons. For trace C, the inset labeled 3_o was obtained by using line broadening larger than that used for the 120 to −60 ppm portion and the spectral intensities of the two traces are not comparable.

to better understand their behavior in solution, we undertook an analysis of their NMR spectra.

Results and Discussion

Figure 1 shows the ^{1}H NMR spectra of (TTP)Fe^{III}(1,4-OC$_6$Cl$_4$O)Fe^{III}(TTP) (trace A) and (TTP)Fe^{III}(1,4-OC$_6$H$_4$O)Fe^{III}(TTP) (trace B) in toluene-d_8 at −30 °C. The spectral patterns are related to those of high-spin ($S = {}^5/_2$), five-coordinate iron(III) porphyrin complexes. Thus pyrrole resonances are seen in the 75–85 ppm region (55–77 ppm at 25 °C). This is slightly upfield of the characteristic region for monomeric high-spin iron(III) complexes (ca. 80 ppm at 25 °C). The meta protons of the *p*-tolyl groups appear as a doublet at 9–11 ppm. The doublet structure occurs as a result of the asymmetry about the porphyrin plane due to the fact that there is only one axial ligand. These two resonances have unequal line widths. This arises because their locations are so different, with one lying on the inside of the dimer, where its relaxation may be affected by both iron centers, and the other lying on the outside, where its relaxation will be dominated by only one iron. The methyl resonance of the *p*-tolyl group appears in the region 4–5 ppm. These resonances have been identified by their relative intensities and by analogy to the spectra of monomeric five-coordinate iron(III) complexes. The resonance at −46 ppm in the spectrum of (TTP)Fe^{III}(1,4-OC$_6$H$_4$O)Fe^{III}(TTP) has no counterpart in the spectrum of (TTP)Fe^{III}(1,4-OC$_6$Cl$_4$O)Fe^{III}(TTP). Hence it arises from the four equivalent protons of the bridging ligand. The chemical shift of this group is readily explicable from what we know about monomeric phenoxy

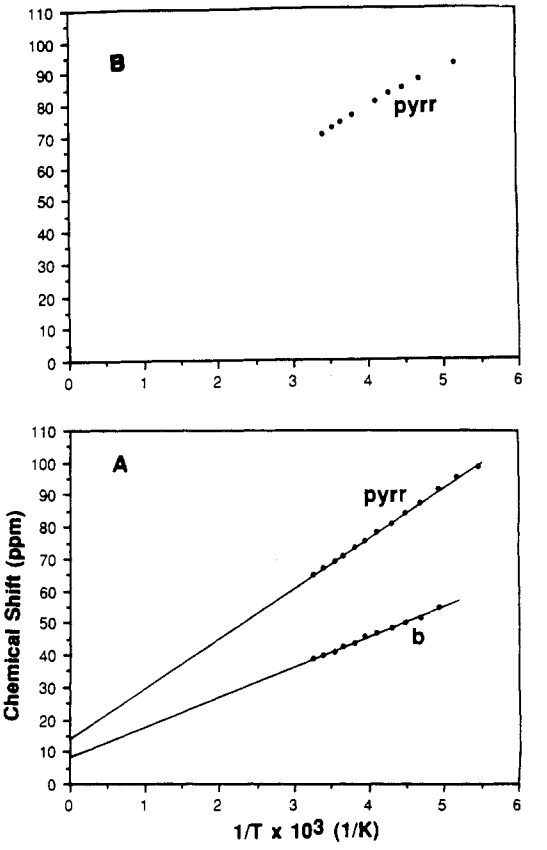

Figure 2. Temperature dependence of the chemical shifts for (A) (TTP)Fe^{III}(1,4-OC$_6$H$_4$O)Fe^{III}(TTP) and (B) (TTP)Fe^{III}(1,4-OC$_6$Cl$_4$O)Fe^{III}(TTP). For the protons of the bridging group in A the absolute value of the chemical shifts (which are negative) are plotted.

Table I. ^{1}H NMR Data for (TTP)Fe^{III}(1,4-OC$_6$R$_4$O)Fe^{III}(TTP) in Toluene-d_8 at 23 °C

	δ, ppm			
bridge	pyrrole	meta	CH_3	bridge
1,4-$O_2C_6H_4$	67.2	9.9 9.4	4.3	−40.2 (H)
1,4-$O_2C_6Cl_4$	70.6	10.5 11.2	4.8	
1,4-O_2C_6(2,3-Cl)(5,6-CN)	73.5	11.1 10.4	5.1	
1,4-$O_2C_6Me_4$	55.3	8.8 9.2	3.8	56.4 (Me)
1,4-$O_2C_6H_2$(2,6-Me)	62.1 63.7	9.2 9.8	4.1 4.2	69.7 (Me)
1,4-O_2C_6H(2,3-MeO)(5-Me)	65.6 66.5	10.3 9.8	4.6 4.8	61.4 (Me)

complexes. For iron(III) phenoxy complexes the ortho protons of the axial ligand generally produce resonances at ca. −120 to −130 ppm while the meta protons produce resonances at ca. 95 ppm. For the bridging ligand in (TTP)Fe^{III}(1,4-OC$_6$H$_4$O)Fe^{III}(TTP), the protons are in a meta position with respect to one iron but are in an ortho position with respect to the other. Hence an upfield shift resonance at ca. −25 to −35 ppm is expected, which is close to the observed chemical shift.

The temperature dependence of the ^{1}H NMR spectra of these two complexes is presented in Figure 2. The plot for the pyrrole hydrogens of (TTP)Fe^{III}(1,4-OC$_6$Cl$_4$O)Fe^{III}(TTP) shows curvature. While curvature in these plots is generally found for high-spin iron(III) porphyrin complexes, the direction of curvature seen here is opposite that seen for monomeric complexes. This is, of course, a result of the antiferromagnetic coupling between the iron centers in these dimers.[2] For (TTP)Fe^{III}(1,4-OC$_6$H$_4$O)Fe^{III}(TTP) the plots for both the pyrrole and bridge protons

(1) Arasasingham, R. D.; Balch, A. L.; Latos-Grażyński, L.; Hart, R. L. *J. Am. Chem. Soc.*, in press.
(2) Kessel, S. L.; Hendrickson, D. N. *Inorg. Chem.* **1980**, *19*, 1883.
(3) Kessel, S. L.; Hendrickson, D. N. *Inorg. Chem.* **1978**, *17*, 2630.
(4) Castro, C. E.; Hathaway, G. M.; Havlin, R. *J. Am. Chem. Soc.* **1977**, *99*, 8032.
(5) La Mar, G. N.; Walker, F. A. *J. Am. Chem. Soc.* **1973**, *95*, 6950.
(6) Walker, F. A.; La Mar, G. N. *Ann. N.Y. Acad. Sci.* **1973**, *206*, 328.
(7) Cheng, R.-J.; Latos-Grażyński, L.; Balch, A. L. *Inorg. Chem.* **1982**, *21*, 2412.
(8) La Mar, G. N.; Eaton, G. R.; Holm, R. H.; Walker, F. A. *J. Am. Chem. Soc.* **1973**, *95*, 63.
(9) Murray, K. S. *Coord. Chem. Rev.* **1974**, *12*, 1.

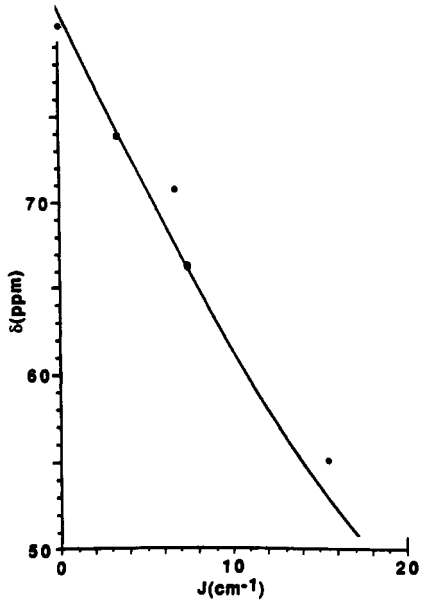

Figure 3. Plot of pyrrole chemical shifts at 23 °C for diiron complexes as a function of the J values obtained from magnetic susceptibility data.[2] The points are experimental data. The solid curve was calculated by using the expression in ref 2 that relates χ_M (the molar susceptibility) and J.

are nearly linear. Again, the deviation from a curved plot seen for the pyrrole shifts of monomeric complexes is caused by the antiferromagnetic coupling, and the linear extrapolations given in this plot show that the intercepts obtained by the Curie law are slightly removed from the positions expected from diamagnetic substances.

Table I presents chemical shift data for a variety of diiron complexes formed by reaction 1. There is a general trend in the pyrrole chemical shifts, which occur higher upfield as the magnitude of the magnetic coupling between the iron ions increases. Figure 3 shows a plot of the pyrrole chemical shifts at 23 °C versus the J values[2] obtained from magnetic susceptibility measured in the solid state. The solid curve was calculated from the published expression relating χ_M (the molar susceptibility) and the J values.[2] Derivation of this curve assumes a proportionality between χ_M and the chemical shift and uses the data for the benzoquinone complex to establish the proportionality constant. From this plot we can estimate J values of compounds for which magnetic susceptibility data are lacking. For example, for the complex obtained from 2,6-dimethyl-1,4-benzoquinone, we estimate J = 9 cm^{-1}.

(TTP)Fe^{III}(1,4-OC_6H_4O)Fe^{III}(TTP) may also be prepared by the reaction of (TTP)$Fe^{III}OFe^{III}$(TTP) with hydroquinone. The reaction of phenols with the μ-oxo species is a well-known route for the synthesis of phenoxy complexes of iron porphyrins.[10] Trace C of Figure 1 shows the results of adding hydroquinone to the μ-oxo species in toluene-d_8. As is typical for this reaction, a mixture of two species is formed. One is (TTP)Fe^{III}(1,4-OC_6H_4O)Fe^{III}(TTP) while the other is (TTP)Fe^{III}(1,4-OC_6H_4OH). The resonance assignments for the latter follow from previous works on related phenolate complexes, which indicate that at 25 °C the ortho protons of coordinated phenoxides appear in the −118 to −131 ppm region and that the corresponding meta protons appear in the 62–94 ppm range with the porphyrin pyrrole protons at ca. 80 ppm.[1,10-13] The monomer (TTP)Fe^{III}(1,4-OC_6H_4OH) is also formed when samples of (TTP)Fe^{III}(1,4-OC_6H_4O)Fe^{III}(TTP) are exposed to water (eq 2).

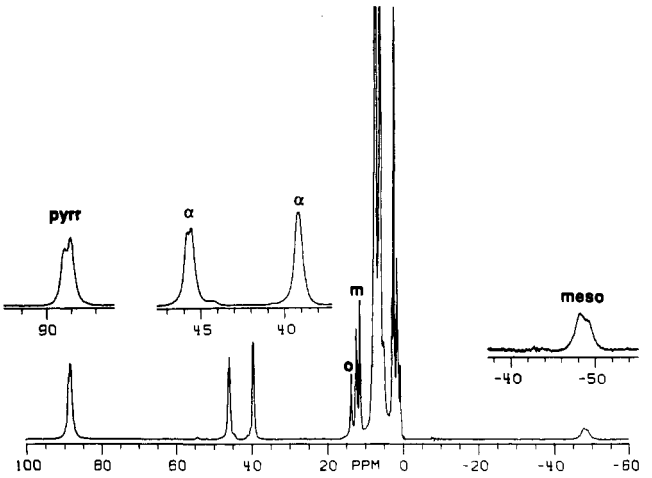

Figure 4. 360-MHz ^1H NMR spectrum at −30 °C of a sample prepared by adding 2,3-dichloro-5,6-dicyano-1,4-benzoquinone to a mixture of (OEP)Fe^{II} and (TTP)Fe^{II} in toluene-d_8. Resonance assignments: pyrr, pyrrole; m, meta (p-tolyl) protons; meso, meso H of OEP; α, methylene H of OEP; o, pyrrole resonance of (TTP)$Fe^{III}OFe^{III}$(TTP).

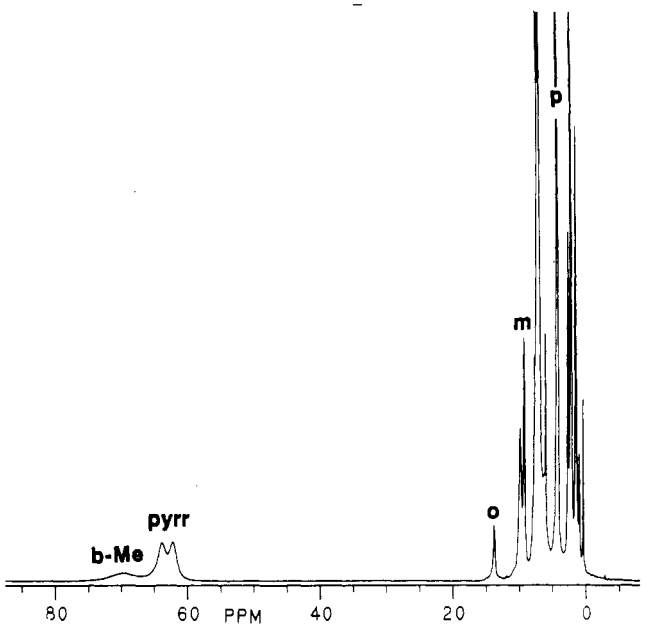

Figure 5. 300-MHz ^1H NMR spectrum of (TTP)Fe^{III}(2,6-Me-1,4-$O_2C_6H_2$)Fe^{III}(TTP) in toluene-d_8 at 22 °C. Resonance assignments: pyrr, pyrrole protons; m, meta (p-tolyl) protons; b-Me, methyl protons of the bridging ligand; p, p-methyl protons of the p-tolyl groups.

(TTP)Fe^{III}(1,4-OC_6H_4O)Fe^{III}(TTP) + H_2O → 2(TTP)Fe^{III}(1,4-OC_6H_4OH) + (TTP)$Fe^{III}OFe^{III}$(TTP) (2)

In order to verify the binuclear nature of these species in solution, we undertook examination of species in which asymmetry was introduced into the structure. Figure 4 shows an experiment in which diiron complexes were prepared with two different porphyrins. The spectrum was obtained by the addition of 2,3-dichloro-5,6-dicyano-1,4-benzoquinone to a mixture of (TTP)Fe^{II} and (OEP)Fe^{II}. Three species, (TTP)Fe^{III}(1,4-$OC_6Cl_2(CN)_2$-O)Fe^{III}(TTP), (OEP)Fe^{III}(1,4-$OC_6Cl_2(CN)_2O$)Fe^{III}(OEP), and (TTP)Fe^{III}(1,4-$OC_6Cl_2(CN)_2O$)Fe^{III}(OEP), are expected to be formed, and indeed, the spectra show evidence for these being present. Thus, there are two pyrrole resonances for the TTP-containing complexes. For the OEP-containing complexes, there are two meso resonances and two resonances for one of the pairs of diastereoptic methylene groups. (The assignments of resonances of the meso and methylene protons of the OEP portion have been

(10) Ainscough, E. W.; Addison, A. W.; Dolphin, D.; James, B. R. *J. Am. Chem. Soc.* **1978**, *100*, 7585.
(11) Goff, H. M.; Shimomura, E. T.; Lee, Y. J.; Scheidt, W. R. *Inorg. Chem.* **1984**, *23*, 315.
(12) Heistand, R. H., II; Lauffer, R. B.; Fikrig, E.; Que, L., Jr. *J. Am. Chem. Soc.* **1982**, *104*, 2789.
(13) Arasasingham, R. D.; Balch, A. L.; Cornman, C. R.; de Ropp, J. S.; Eguchi, K.; La Mar, G. N. *Inorg. Chem.* **1990**, *29*, 1847.

verified by independently observing the spectrum of (OEP)-$Fe^{III}(1,4\text{-}OC_6Cl_2(CN)_2O)Fe^{III}$(OEP).) These features are emphasized in the insets in Figure 4. These observations assure us that the species being observed in these NMR spectra are the intact, dimeric species. Additionally, we have noted that there is no concentration dependence of these spectra, whereas dissociation should produce concentration effects.

Asymmetry can also be introduced into these species by employing an unsymmetrical quinone. Figure 5 shows the spectrum obtained by using reaction 1 with 2,6-dimethyl-1,4-benzoquinone (R, R'' = H; R', R''' = CH_3). The spectrum clearly shows two equally intense pyrrole resonances at 62 and 64 ppm along with a broad resonance at 70 ppm due to the methyl groups of the bridging ligand. The other two protons of that bridge were not seen; presumably they were too broad. Similarly, splitting of the pyrrole resonances was also observed with the diiron complex formed from 2,3-dimethoxy-5-methyl-1,4-benzoquinone (coenzyme Q_0; R, R' = OMe, R'' = Me, R''' = H).

Experimental Section

Materials. Substituted quinones were obtained from Aldrich Chemicals, and the diiron complexes were obtained via reaction 1 according to the method of Kessel and Hendrickson.[2] The sample used to obtain the spectrum shown in trace C of Figure 1 was prepared by heating a mixture of (TTP)$Fe^{III}OFe^{III}$(TTP) and excess *p*-hydroquinone in toluene-d_8 for 1 h at 80 °C in an NMR tube.

Instrumentation. NMR spectra were recorded on Nicolet NT-360 FT and GE QE-300 spectrometers operating in the quadrature mode (^1H frequencies are 360 and 300 MHz, respectively). The spectra were collected over a 40-kHz bandwidth with 16K data points and a 6-μs 90° pulse. For a typical paramagnetic spectrum, between 500 and 2000 transients were accumulated with a delay time of 50 ms. The signal-to-noise ratio was improved by apodization of the free induction decay. The residual methyl peak of toluene was used as a secondary reference, which was set at 2.09 ppm.

Acknowledgment. We thank the National Institutes of Health (Grant GM-26226) for support.

Registry No. (TTP)$Fe^{III}(1,4\text{-}O_2C_6H_4)Fe^{III}$(TTP), 128471-79-4; (TTP)$Fe^{III}(1,4\text{-}O_2C_6Cl_4)Fe^{III}$(TTP), 128471-80-7; (TTP)$Fe^{III}(1,4\text{-}O_2C_6(2,3\text{-}Cl)(5,6\text{-}CN))Fe^{III}$(TTP), 128471-81-8; (TTP)$Fe^{III}(1,4\text{-}O_2C_6Me_4)Fe^{III}$(TTP), 128471-82-9; (TTP)$Fe^{III}(1,4\text{-}O_2C_6H_2(2,6\text{-}Me))Fe^{III}$(TTP), 128471-83-0; (TTP)$Fe^{III}(1,4\text{-}O_2C_6(2,3\text{-}MeO)(5\text{-}Me))Fe^{III}$(TTP), 128471-84-1.

Contribution from the Department of Chemistry, National Taiwan University, Taipei, Taiwan, ROC

Charge Density Study of Thiourea *S,S*-Dioxide

Yu Wang,* Ning-Leh Chang, and Ching-Tzong Pai

Received October 3, 1989

Thiourea *S,S*-dioxide has been studied by X-ray diffraction at room temperature.[1,2] The unusually long carbon–sulfur bond was noticed,[1] and a suggestion of mesoionic character with a positive charge located on the $(NH_2)_2C$ part and a negative charge on the SO_2 part of the molecule was made.[1] Dunitz[3] gave an explanation that the weakening of the carbon–sulfur p_σ–p_σ bond[1,3] is due to the odd electron of SO_2^- being of d_π character. In order to understand the bonding character of this molecule, a deformation density study was undertaken. The same approach was applied to the thiourea molecule, where the electron density distribution was studied both experimentally and theoretically in detail.[4-8] It would be a nice comparison between thiourea and thiourea dioxide to see the difference in the C–S bond as well as in the long-pair region of the sulfur atom. The strong hydrogen bonds in this crystal are also of interest.

* To whom correspondence should be addressed.

Table I. Crystal Data for Thiourea *S,S*-Dioxide

chem formula	$(H_2N)_2CSO_2$	fw	110
a, Å	10.719 (2)	space group	*Pnma* (No. 62)
b, Å	10.109 (2)	μ, cm^{-1}	6.10
c, Å	3.8018 (7)	λ, Å	0.7107
D_{calcd}, $g\cdot cm^{-3}$	1.743	transm coeff	0.74–0.89
V, $Å^3$	411.9	$R(F)$	0.0225, 0.0183[a]
Z	4	$R_w(F)$	0.0363, 0.0233[a]
T, K	110		

[a] High-order refinement.

Table II. Atomic Fractional Coordinates and B(eq) ($Å^2$)

atom	refinement	*x*	*y*	*z*	B(eq)[d]
S	*a*	0.460 52 (1)	0.25	0.361 01 (4)	0.827 (5)
	b	0.460 54 (8)	0.25	0.361 06 (3)	0.811 (4)
	c	0.460 55 (1)	0.25	0.361 05 (2)	0.810 (3)
C	*a*	0.611 62 (4)	0.25	0.601 19 (15)	0.818 (12)
	b	0.611 67 (3)	0.25	0.601 29 (11)	0.799 (8)
	c	0.611 68 (3)	0.25	0.601 30 (10)	0.809 (9)
N	*a*	0.663 61 (3)	0.364 77 (3)	0.664 77 (11)	1.082 (10)
	b	0.663 57 (2)	0.364 70 (3)	0.664 71 (8)	1.070 (6)
	c	0.663 59 (2)	0.364 63 (3)	0.664 85 (9)	1.071 (7)
O	*a*	0.401 79 (3)	0.127 48 (3)	0.509 54 (10)	1.093 (9)
	b	0.401 73 (2)	0.127 67 (2)	0.509 68 (7)	1.074 (6)
	c	0.401 73 (2)	0.127 58 (3)	0.509 60 (9)	1.074 (7)
H1	*a*	0.737 0 (7)	0.369 6 (9)	0.768 (3)	1.78 (16)
	b	0.746 92	0.370 23	0.781 97	1.78
H2	*a*	0.628 8 (7)	0.432 2 (11)	0.626 5 (24)	1.72 (17)
	b	0.619 64	0.450 05	0.616 36	1.72

[a] From full data refinement. [b] From high-angle data ($(\sin\theta)/\lambda > 0.65$) refinement. [c] From multipole refinement. [d] $B(eq) = (8/3)\pi^2\sum_i\sum_j(i,j)a_i^*a_j^*\cdot a_i a_j$.

Experimental Section

The title compound was prepared by oxidizing thiourea with 3% hydrogen peroxide at 0 °C for 3 h and crystallized in an aqueous solution.

The crystal data of $(NH_2)_2CSO_2$ at 110 K are listed in Table I. The intensity data were collected on a CAD4 diffractometer equipped with a graphite monochromator and liquid-N_2 gas flow set up using Mo Kα radiation. A sealed box was designed[9] with a dry ice/acetone cold trap to ensure a low humidity around the crystal. Some of the experimental details are given in Table I. The intensity data were measured up to $2\theta = 100°$ for two equivalent sets of reflections (hkl, $\bar{h}kl$). Five measurements at ψ values from −30 to 30° with a step of 15° were collected for each reflection up to $2\theta = 60°$. An additional equivalent set of reflections ($hk\bar{l}$) was collected up to $2\theta = 90°$. This yielded a total of 8676 measurements, which gave 2224 unique reflections after averaging of equivalents. The interest agreement is 2.1%. Three standard reflections monitored every 1 h showed variations of less than ±5%. An absorption correction was applied according to 10 measured faces of the compound. The crystal size is large in one direction, but cutting of the crystal would cause crystal damage. The collimator size was adjusted to ensure that the crystal was in the beam. All of the computations were carried out on a local MicroVAXIII computer using mainly NRCVAX programs.[10] The refinements of the multipole model were also carried out on the MicroVAX computer using the MOLLY program.[11] Both least-squares refinements are based on F_o, with weight calculated as $1/[\sigma^2(F_o) +$

(1) Sullivan, R. L.; Hargreaves, A. *Acta Crystallogr.* **1962**, *15*, 675.
(2) Chen, I. C.; Wang, Y. *Acta Crystallogr., Sect. C: Cryst. Struct. Commun.* **1984**, *C40*, 1890.
(3) Dunitz, J. D. *Acta Crystallogr.* **1956**, *9*, 579.
(4) Mullen, D.; Hellner, E. *Acta Crystallogr., Sect. B: Struct. Crystallogr. Cryst. Chem.* **1978**, *B34*, 2789.
(5) Mullen, D.; Scheringer, C. *Acta Crystallogr., Sect. A: Cryst. Phys., Diffr., Theor. Gen. Crystallogr.* **1978**, *A34*, 476.
(6) Kutoglu, A.; Scheringer, C.; Meyer, H.; Schweig, A. *Acta Crystallogr., Sect. B: Struct. Sci.* **1982**, *B38*, 2626.
(7) Breitenstein, M.; Dannohl, H.; Meyer, H.; Schweig, A.; Seeger, R.; Seeger, U.; Zittlau, W. *Intl. Rev. Phys. Chem.* **1983**, *3*, 335.
(8) Mullen, D. *Acta Crystallogr., Sect. B: Struct. Sci.* **1982**, *B38*, 2620.
(9) Ueng, C. H. Ph.D. Thesis, National Taiwan University, 1987.
(10) Gabe, E. J.; Lee, F. L.; LePage, Y. *Crystallographic Computing 3*; Sheldrick, G. M., Kruger, C., Goddard, R., Eds.; Clarendon Press: Oxford, England, 1985; pp 167–174.
(11) Hansen, N. H.; Coppens, P. *Acta Crystallogr., Sect. A: Cryst. Phys., Diffr., Theor. Gen. Crystallogr.* **1978**, *A34*, 909.

0020-1669/90/1329-3256$02.50/0